Am J Physiol Regul Integr Comp Physiol 299: R000 –R000, 2010.
First published May 12, 2010; doi:10.1152/ajpregu.00699.2009.

Gas embolization of the liver in a rat model of rapid decompression

AQ: 2

Antonio L'Abbate,[1,2] Claudia Kusmic,[3] Marco Matteucci,[1] Gualtiero Pelosi,[3] Alessandro Navari,[4] Antonino Pagliazzo,[3] Pasquale Longobardi,[5] and Remo Bedini[2,3]

[1]*Scuola Superiore Sant'Anna, Pisa,* [2]*Extreme Centre of Scoula Superiore Sant'Anna,* [3]*Istituto di Fisiologia Clinica del Consiglio Nazionale delle Ricerche, Pisa, and* [4]*Fondazione Toscana Gabriele Monasterio, Pisa, Italy;* [5]*Centro Iperbarico, Ravenna, Italy*

Submitted 26 October 2009; accepted in final form 9 May 2010

L'Abbate A, Kusmic C, Matteucci M, Pelosi G, Navari A, Pagliazzo A, Longobardi P, Bedini R. Gas embolization of the liver in a rat model of rapid decompression. *Am J Physiol Regul Integr Comp Physiol* 299: R000 –R000, 2010. First published May 12, 2010; doi:10.1152/ajpregu.00699.2009.—Occurrence of liver gas embolism after rapid decompression was assessed in 31 female rats that were decompressed in 12 min after 42 min of compression at 7 ATA (*protocol A*). Sixteen rats died after decompression (*group I*). Of the surviving rats, seven were killed at 3 h (*group II*), and eight at 24 h (*group III*). In *group I*, bubbles were visible in the right heart, aortic arch, liver, and mesenteric veins and on the intestinal surface. Histology showed perilobular microcavities in sinusoids, interstitial spaces, and hepatocytes. In *group II*, liver gas was visible in two rats. Perilobular vacuolization and significant plasma aminotransferase increase were present. In *group III*, liver edema was evident at gross examination in all cases. Histology showed perilobular cell swelling, vacuolization, or hydropic degeneration. Compared with basal, enzymatic markers of liver damage increased significantly. An additional 14 rats were decompressed twice (*protocol B*). Overall mortality was 93%. In addition to diffuse hydropic degeneration, centrilobular necrosis was frequently observed after the second decompression. Additionally, 10 rats were exposed to three decompression sessions (*protocol C*) with doubled decompression time. Their mortality rate decreased to 20%, but enzymatic markers still increased in surviving rats compared with predecompression, and perilobular cell swelling and vacuolization were present in five rats. Study challenges were *1*) liver is not part of the pathophysiology of decompression in the existing paradigm, and *2*) although significant cellular necrosis was observed in few animals, zonal or diffuse hepatocellular damage associated with liver dysfunction was frequently demonstrated. Liver participation in human decompression sickness should be looked for and clinically evaluated.

AQ:3

decompression sickness; gas embolism; diving; liver dysfunction; hyperbaric chamber

ACCORDING TO GAS LAWS WHEN the body is exposed to increased hydrostatic pressure, as occurs during diving, gas phases are forced to go into solution in body fluids. As the diver descends, the increased pressure causes more nitrogen to dissolve into tissue fluids. This is particularly important for long-lasting dives, as in the case of scuba divers. Upon ascent, if the diver returns to the surface too quickly, the excess gas, while in solution in the blood, will not have the chance to be gradually eliminated through the lungs but will go into a gas phase (bubbles) in both tissues and blood.

Bubbles entering the blood at the level of microcirculation flow through the systemic veins to the right heart and embolize in the lungs. From the lung microcirculation, bubbles can lose their gas content in the alveolar spaces or, in some adverse circumstances, reach the left heart and the systemic arterial circulation with dramatic clinical complications, such as ischemia or necrosis of embolized tissues. The trapping of autochthonous bubbles in tissues can also produce injury. These unfavorable outcomes of rapid decompression are components of decompression sickness (DCS), which is treated with recompression in the hyperbaric chamber (6, 23).

Considerable literature is available on bubble embolism in both pulmonary and arterial circulations following decompression. In contrast, few mentions can be found of gas microbubbles traveling through the third largest circulatory system in the body, namely the portal vein circulation, which transports venous blood from the splanchnic organs to the liver. Marginal and contradictory findings on portal, mesenteric, liver, and spleen gas bubbles are only reported in old experimental studies on dysbarism or in occasional case reports (1, 4, 23). Similarly, abnormal blood markers of liver dysfunction have been occasionally reported in divers (15, 20). In conclusion, the common view is that the liver is not a target organ of DCS.

Apparently there is no physiological reason for the exclusion of the portal vein system from participating in the process of bubble formation and delivery. On the contrary, some peculiarities of the portal circulation make this a vascular area of particular interest for the study of diving physiopathology.

The first peculiarity is that bubbles originating in the intestinal microcirculation do not travel directly to the systemic venous circulation, as occurs for all bubbles originating in any other organ, but instead reach the liver microvascular filter. In this instance, only bubbles escaping from the liver sinusoids or bypassing them via preexisting portocaval collateral veins will eventually reach the pulmonary circulation. One possible reason for the supposed negligible involvement of the liver in DCS might be inadequate liver embolization due to loose microvascular filtering. However, this view has never been supported by experimental testing.

The second peculiarity is related to the presence of gas in the bowel and to the special condition of the intestinal wall tissue that interfaces blood on one side and intestinal gas on the other. This condition is not unlike the one in the lung where gases contained in the blood, tissue, and alveolar spaces move along the three compartments according to the gas laws (Fig. 1). F1

Thus, if sequestered in a closed intestinal segment, intestinal gas will dissolve into the surrounding tissue according to the increased hydrostatic pressure during diving and to the partial pressure and diffusion coefficient of its components. It is worthy to note that intestinal gas in rats on the usual laboratory diet, has been shown to be composed by the same gases present in the air but in different proportions and thus with different partial pressures (12). In this situation, the intestinal tissue wall

Address for reprint requests and other correspondence: C. Kusmic, CNR Institute of Clinical Physiology, Via G Moruzzi 1, 56124 Pisa, Italy (e-mail:kusmic@ifc.cnr.it).

AQ: 8

tapraid4/zh6-areg/zh6-areg/zh600810/zh67282d10z | xppws | S 1 | 5/26/10 | 2:44 MS: R-00699-2009 Ini: 08/bar/ss

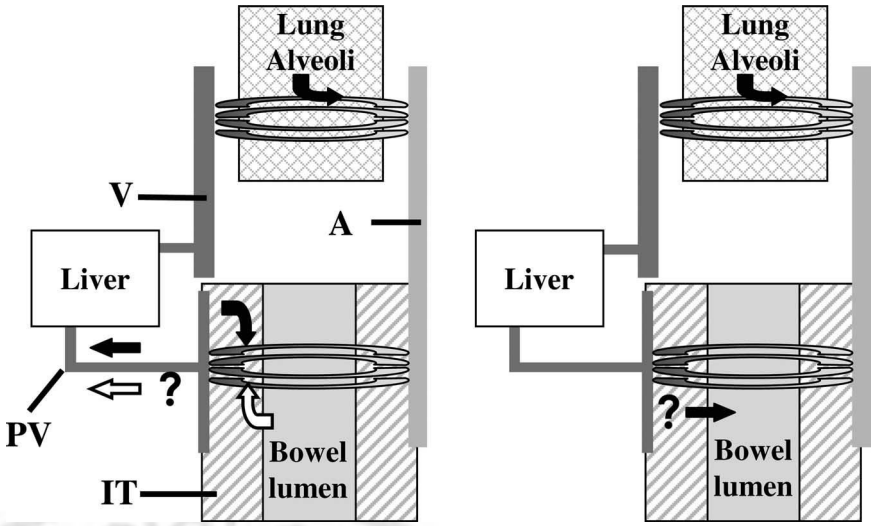

Fig. 1. Schematic representation of tissue-blood gas exchange in the intestine. Two hypotheses are compared: intestinal gas contributes to liver embolization (white arrows, *left*) or the respiratory gas saturating the intestinal wall escapes into the bowel lumen (black arrow, *right*), thus protecting the liver from gas embolization. A, systemic arterial circulation; V, systemic venous circulation; PV, portal venous circulation; IT, intestinal wall tissue.

will contain a mixture of both respiratory and intestinal gases, which, upon ascent, will move toward the portal circulation or toward the bowel lumen according to respective partial pressure gradients. Thus, a second reason for the supposedly negligible involvement of the liver in DCS could be the escape of gas from the saturated intestinal wall to the intestinal lumen. In this case, the liver would be protected by the intestinal cavity, which would work as the lung does for the systemic circulation. However, once again, this supposition is not supported by experimental data.

In this study, we investigated the hypothesis that, after decompression and similar to the systemic venous circulation, gas bubbles form in the splanchnic organs, move into the portal vein, and embolize in the liver, with possible consequent hepatic dysfunction.

Moreover, we investigated liver abnormalities secondary to single as well as to repeated decompressions.

MATERIALS AND METHODS

Animals and Experimental Protocol

Our experimental protocols were approved by the Animal Care Committee of the Italian Ministry of Health and conformed to the "Guiding Principles for Research Involving Animals and Human Beings" approved by the Council of the American Physiological Society.

We studied a total of 63 adult female Wistar rats aged 6 –9 mo and weighing 275 40 g (range, 220 –370 g). Female rats were chosen because of the higher fat-to-muscle ratio compared with males, which is an important factor in gas dissolution in tissue fluids.

Animals were housed under controlled 12:12-h light-dark cycle, temperature (21 0.5°C), and relative humidity (55% 2%) in animal rooms. Rats were fed with 4RF18 pelleted rodent diet for long-term maintenance (Mucedola, Italy) and water ad libitum until 1 h before the experiments.

Of the 63 rats studied, 55 were compressed (simulated dive) in a hyperbaric chamber, usually in pairs, but housed in single cages. The remaining eight rats were not compressed in the hyperbaric chamber and represented the control group for gross anatomy and histological liver examination.

Study design envisaged three decompression protocols. In *protocol A*, 31 rats were compressed to 7 ATA and after 42 min, were rapidly (12 min) decompressed. In *protocol B*, to investigate the effects of repeated decompressions, we exposed 14 rats, 48 h apart, to two decompression sessions with the same diving profile as in *protocol A*. In *protocol C*, 10 rats were exposed, 48 h apart, to three decompression sessions by using a mitigated diving profile (see below).

Hyperbaric Chamber Characteristics and Profile of Simulated Dive

The experimental chamber was a 50-liter homemade compression chamber (OMASA, Rome, Italy) that simulated dry and humid hyperbaric conditions up to 12 ATA (1,216 kPa). The chamber's operating monitor was equipped with one input pressure aneroid manometer (Wika 39.4 ATA max, class 0.25) and one large-screen aneroid manometer (Wika 24.6 ATA max class 0.25). The chamber was prepared with internal illumination and two video cameras for visual monitoring of the animals during compression and decompression periods (Fig. 2). A personal computer was connected to internal sensors to monitor both pressure and temperature and to record animal video imaging. A scuba-diving bottle containing 18 liters at 200 ATA (20,165 kPa) of air was used to fill the chamber by means of a standard first stage scuba regulator that provides a constant 10 ATA (2,016 kPa) source of air. The experimental immersion profile was obtained manually by simply operating the inflating-deflating lockgates; in particular, the compression was controlled by monitoring the pressure inside the chamber, while the decompression was assured by a constant deflating flow monitored by a Pitot tube flowmeter. F2

In *protocols A* and *B* animals were compressed at a rate of 2 ATA (203 kPa)/min to a final pressure of 7 ATA (709 kPa, 60 water meters) and kept at that pressure for 42 min while breathing air. At the end of the compression period, rats were almost linearly decompressed to the surface, i.e., 1 ATA (101 kPa), at a rate of 0.5 ATA (51 kPa)/min in 12 min.

Using the above protocol, Wisloff and Brubakk (26) were able to reproducibly induce DCS and bubbles, as documented by echo imaging of the right heart, in rats surviving early death.

In rats exposed to three decompression sessions (*protocol C*), the diving profile was mitigated, doubling the decompression time to 24 min, while the other variables remained constant.

Enzymatic Markers of Liver Damage

Heparinized blood samples were obtained from the femoral vein of animals subjected to decompression protocol. A blood sample was collected before simulated diving (basal) and at 3 and 24 h in the surviving rats in *protocol A* and at 24 h after each decompression in *protocols B* and *C*. Plasma was assayed for concentrations of aspartate aminotransferase (AST), alanine aminotransferase (ALT), -glutamyl transferase (GGT), lactate dehydrogenase (LDH), and creatinine ki-

tapraid4/zh6-areg/zh6-areg/zh600810/zh67282d10z | xppws | S 1 | 5/26/10 | 2:44 MS: R-00699-2009 Ini: 08/bar/ss

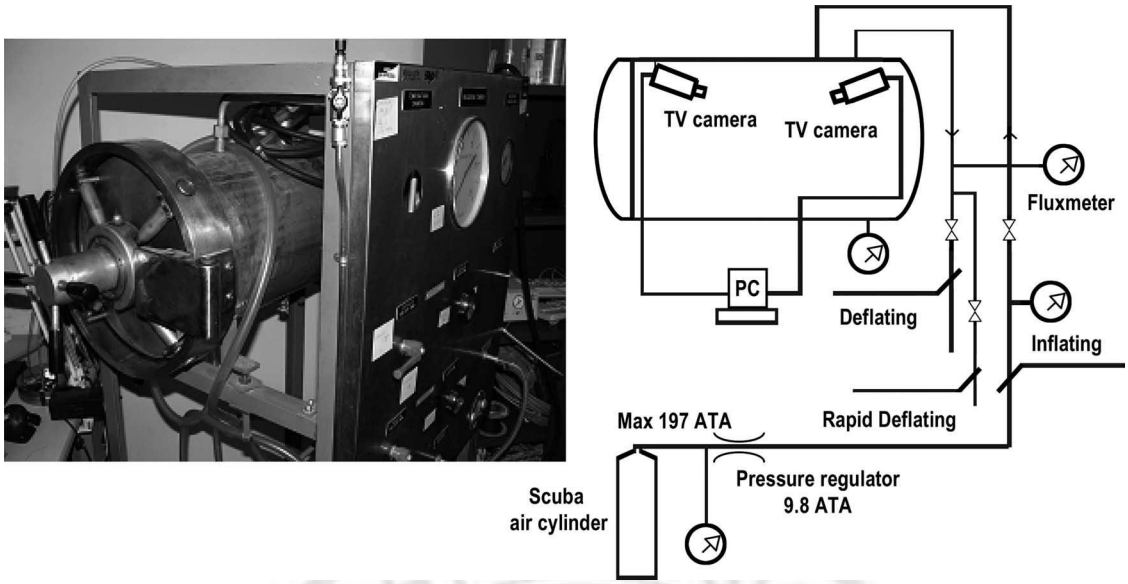

Fig. 2. *Left*: the experimental 50-liter homemade hyperbaric chamber. *Right*: schematic representation of the technical arrangement.

nase (CK) by routine laboratory methods using a CX9PRO autoanalyzer (Beckman Coulter, Sykesville, MD).

Gross Morphology and Microscopy

After early spontaneous death or death at 3 or 24 h, each rat's abdomen was incised, and liver and intestine were exposed for gross examination and digital photography. The right lobe of the liver was transversally sectioned to examine the internal gross appearance, and the mesentery was distended to visualize blood vessels. The chest was then opened to explore gas content in the right heart and aortic arch.

Four samples from the right and median lobes from each liver were excised, rinsed in physiologic solution, fixed in 10% phosphate-buffered formalin for 4 days, and then embedded in paraffin. Additional samples were also collected for liquid nitrogen freezing. From the paraffin-embedded tissue blocks, 5- m to 6- m sections were obtained. Four to eight sections of each liver were stained with hematoxylin and eosin. Additionally, adjacent serial sections stained for hepatic glycogen with periodic acid Shiff (PAS) staining were examined. Tissue sections, following Tissue Tek (Sakura Finetek, Europe) inclusion and liquid nitrogen freezing, were also processed in the cryomicrotome for red oil staining (lipid specific stain). All sections were examined at 100, 200, and 400 magnification under light microscopy (Leitz Orthoplan, Germany, interfaced to an Olympus DP 20 digital acquisition system, Japan) by two independent blinded observers. Categorized histological alterations (see RESULTS) were semiquantitatively scored as mild (focal), moderate (zonal), and severe (diffuse, bridging the lobules). Tissue density of stainless microcavities (air microbubbles) was expressed as mean SE number of vacuoli per 100 m in at least 10 fields of each liver specimen.

In four animals from *group I* (early spontaneous death), in *protocol A*, histological examination of the spleen was also performed.

Statistical Analysis

Data are expressed as means SE. Statistical significance of differences between groups was determined by ANOVA followed by post hoc Dunnett's test or by paired and unpaired Student's *t*-test as appropriate. A probability (P) value of 0.05 was considered statistically significant.

RESULTS

Animal Survival

In *protocol A*, out of the 31 decompressed rats, 16 died within 1 h after decompression (52% mortality). Of these, 14 rats (88%) died within 10 min, while the remaining two died between 20 and 40 min (*group I*, *n* 16). Of the 15 surviving animals, seven were randomly selected and killed by an anesthetic overdose (pentobarbital sodium at 200 –250 mg/kg ip) at 3 h after decompression (*group II*, *n* 7). The remaining eight animals were returned to the cage and killed at 24 h (*group III*, *n* 8). There were no spontaneous deaths between 3 and 24 h.

In *protocol B*, out of 14 rats exposed to two decompression sessions, seven died after the first decompression, in agreement with the results of *protocol A*, and six died after the second decompression (overall mortality rate 93%). In contrast, in *protocol C*, out of 10 rats exposed to a milder decompression profile compared with *protocols A* and *B*, eight survived to three decompression cycles (20% overall mortality rate).

Enzymatic Markers of Liver Dysfunction

Changes in plasma enzymatic markers of liver dysfunction in surviving animals, relative to their own basal values (intra-animal comparison) are reported in Table 1. T1

In *protocol A*, the simulated dives induced significant increases, relative to basal condition, in AST at 3 h and 24 h after decompression and in ALT and GGT at 24 h only. CK and LDH did not change significantly.

In rats exposed to three decompression sessions (*protocol C*) with the modified (less severe) diving profile, AST and ALT values increased significantly at 24 h after each decompression session relative to basal values, as also reported in Table 1. Conversely GGT, CK, and LDH did not change significantly.

Postmortem Gross Examination

Control cases all showed normal anatomy of liver, intestine, and mesenteric veins.

tapraid4/zh6-areg/zh6-areg/zh600810/zh67282d10z | xppws | S 1 | 5/26/10 | 2:44 MS: R-00699-2009 Ini: 08/bar/ss

Table 1. *Hematochemical markers of liver function*

	n	AST		ALT		GGT		LDH		CK	
					Protocol A						
Basal	15	54	2	27	1	4	1	774	79	152	16
3 h postdecompression	15	105	14*	28	4	5	1	1130	155	169	16
24 h postdecompression	8	159	26*	53	13*	12	3*	718	142	172	32
					Protocol C						
Basal	8	49	3	27	4	4	2	329	38	185	24
24 h postdecompression *group I*	8	333	123*	81	23*	8	2	602	193	275	82
24 h postdecompression *group II*	8	133	36*	35	4*	7	2	439	219	294	167
24 h postdecompression *group III*	8	77	10*	45	8*	7	1	319	86	170	32

Values are means SE in units/liter; *n*, number of animals tested. AST, aspartate aminotransferase; ALT, alanine aminotransferase; GGT, -glutamyl transferase; LDH, lactate dehydrogenase; CK creatine kinase. *P 0.05 vs. basal values.

Protocol A. *GROUP I* (SPONTANEOUS EARLY DEATH). At autopsy, all of the animals in this group showed a swollen, spongy liver of normal color. The organ was soft, and when cut, a considerable amount of bloody foam emerged at the surface as micro- and macrobubbles that clustered and dissolved on the cut surface. Multiple large gas bubbles were also evident on the intestine surface under the peritoneal membrane and within intestinal and mesenteric veins in all cases (Fig. 3*A*). Gas was also evident by transparency in the inferior vena cava, right heart, pulmonary artery, and, as shown in Fig. 4, in the aortic arch. No gas bubbles were perceived when the spleen was cut.

GROUP II. In surviving animals killed at 3 h, the liver appeared of normal color and normal tissue consistency in all cases. However, when sectioned, a small amount of gas bubbles emerged and dissolved on the cut surface in two out of seven cases. Bubbles in the mesenteric veins were seldom observed (Fig. 3*B, right*), while no gas bubbles were visible on the intestine surface nor in the inferior vena cava, right heart, or aortic arch.

GROUP III. All surviving animals killed 24 h after decompression showed a swollen, apparently edematous, liver at autopsy. Color was normal in four cases and pale in four; in all cases,

COLOR

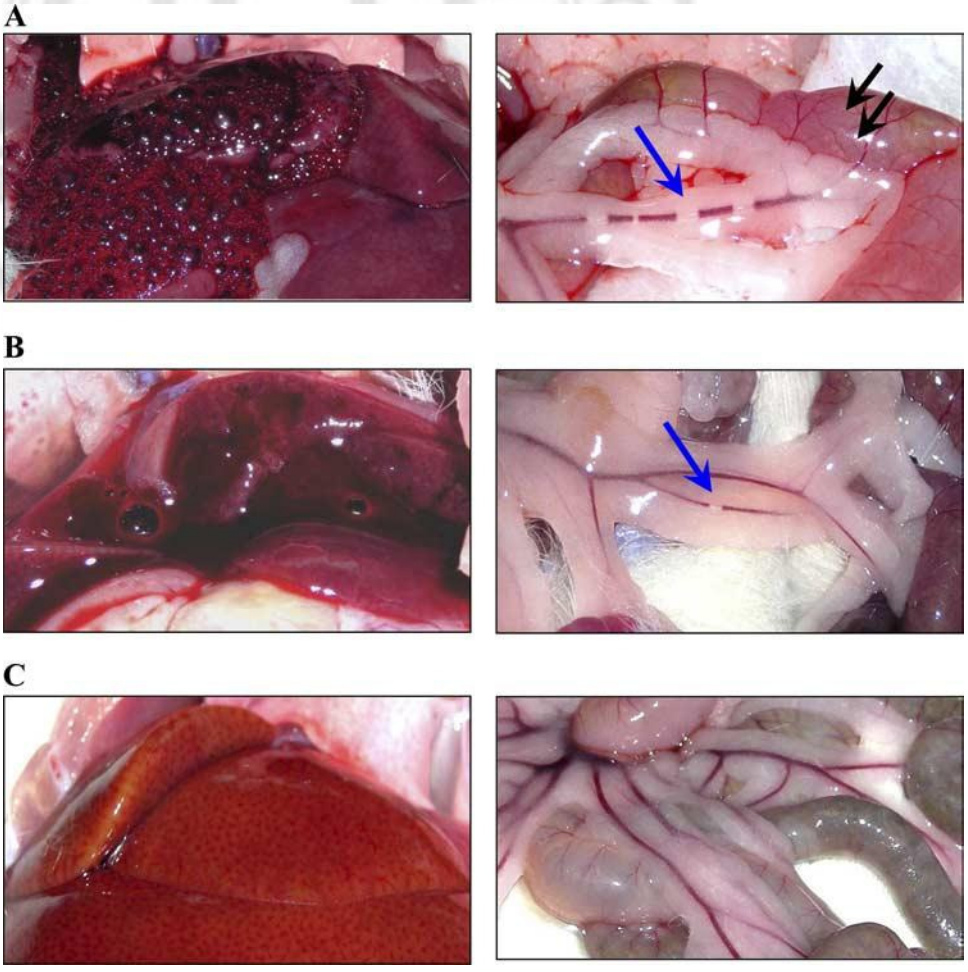

Fig. 3. *Protocol A*. Gross morphology of liver, intestine, and mesenteric veins in a control animal and in 3 representative cases from *groups I*, *II*, and *III*, respectively (*A–C*). *A*: severe gas embolism of the liver (*left*) is evident as bloody foam at the cut surface; bubbles are present in the intestine wall (*right*, black arrows) as well as in a mesenteric vein, as a series of empty spaces (*right*, blue arrow). *B*: residual bubbles dissolve at the cut surface of the liver (*left*), and a single empty space can be seen in a mesenteric vein (*right*, blue arrow). *C*: a swollen, pale liver with a fishnet appearance on the surface is evident, indicating severe edema (*left*) with moderate congestion of mesenteric veins (*right*).

tapraid4/zh6-areg/zh6-areg/zh600810/zh67282d10z | xppws | S 1 | 5/26/10 | 2:44 MS: R-00699-2009 Ini: 08/bar/ss

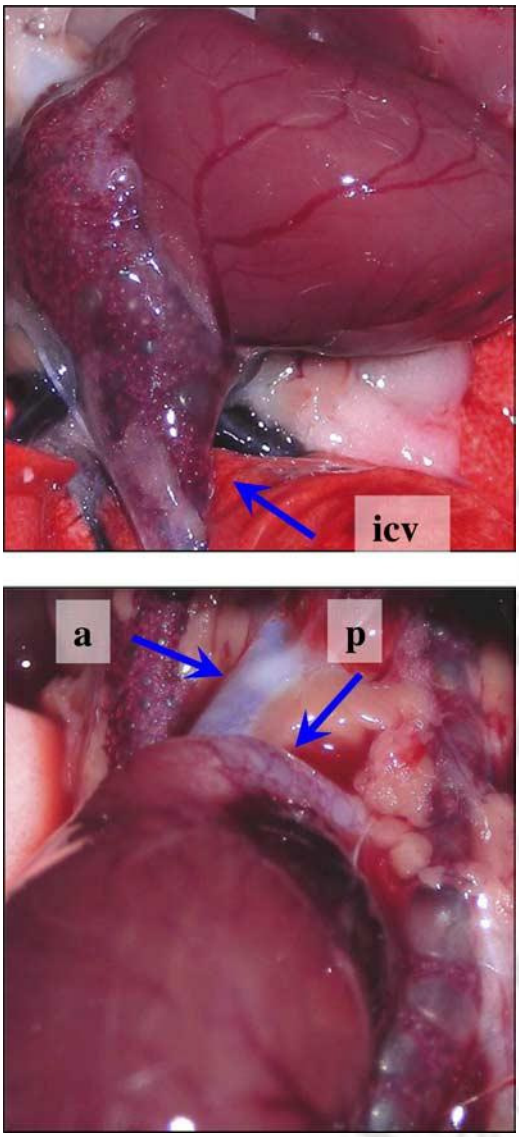

Fig. 4. Enlarged photographs of the thoracic cavity of a rat that died a few minutes after the decompression procedure (*protocol A*, *group I*). The massive presence of gas bubbles can be seen as a transparency in the inferior vena cava (icv, blue arrow), the right atrium, the pulmonary artery (p, blue arrow), and in the aortic arch (a, blue arrow).

COLOR

the lobules were clearly visible on the surface, as outlined by a dark perilobular contour, with a resulting trabecular fishnet pattern (Fig. 3*C, left*). No gas bubbles were macroscopically apparent in the liver, intestine, and mesenteric veins or in the right heart.

Protocol B. In the rats who died spontaneously after the second decompression session, gross examination of the liver and intestine showed extensive gas embolism as in *group I* animals of *protocol A*; gas bubbles were invariably present in the inferior vena cava, right heart, pulmonary artery, and aortic arch. In the only surviving rat of this series, massive liver edema, subcapsular gas bubbles, and the loss of the trabecular lobular pattern were evidenced.

Protocol C. In the two rats that died spontaneously during the repeated decompression protocol with the modified diving profile, we observed the same distribution of gas embolism as in *group I* animals of *protocol A*, although with less and smaller bubbles. Finally, in the surviving rats of *protocol C*, we found a normal gross anatomy of liver and intestine.

Liver Histology and Histochemistry

Controls. Normal lobular architecture with preserved hepatocellular morphology was present in all cases with few red blood cells in the central veins, portal veins, and sinusoids.

Protocol A. GROUP I. Two distinct histological features were present in the seven cases processed for microscopic examination. Out of the 16 nonsurviving animals we found *1*) enlarged sinusoids and central venules filled with packed red cells and sinusoids containing empty spaces of irregular or cylindrical shape in correspondence with dilated segmental profile; and *2*) round, unstained cavities 2–20 m in diameter, both within and outside of the hepatocytes, consistently located in the perilobular zone with an average tissue density of 25 7 vacuoli/100 m^2. All microcavities failed to stain with hematoxylin and eosin, PAS, and red oil. This feature suggests the gaseous nature of the microcavities, at least for those contained in the sinusoids, while for the others (in the perilobular interstitium or in the hepatocytes), water content (hydropic vacuolization) cannot be categorically excluded. In the high microcavities, tissue density of all cases, however, was not associated with significant cellular injury, with the exception of a single case of centrilobular hydropic degeneration associated with massive (40 10 vacuoli/100 m^2) perilobular vacuolization (Fig. 5*A*). PAS staining for hepatic glycogen was either totally negative or positive only in single centrilobular cells, while red oil was consistently negative (Fig. 6*A*). F5, AQ:5 F6

Histological examination of the spleen in four animals of this group did not evidence any pattern suggestive of autochthonous gas microbubble formation (data not shown).

GROUP II. Extra- and intracellular vacuolization with the same characteristics described above was also present in all cases surviving 3 h after decompression. Unstained microcavities showed a strictly perilobular zonation with a lower tissue density (14 5 vacuoli/100 m^2) than in *group I* (Fig. 5*B*). Lobular architecture was intact, moderate cellular swelling was present, and sinusoids and portal veins appeared congested with red blood cells. PAS and red oil stains were both negative (Fig. 6*B*).

GROUP III. Two distinct histological patterns were observed: *1*) zonal (perilobular) cell swelling and vacuolization with PAS negative stain in four cases; and *2*) hydropic degeneration, either massive, with no zonal distribution, or prominently mid- and centrilobular, with collapsed sinusoids and compressed central veins, few cellular foci of PAS, and red oil positive stains in four cases. Nuclear morphology was generally normal (no karyolysis or picnosis), plasma membrane was intact, and lobular architecture preserved. No significant cellular necrosis was detected: neither ballooning degeneration nor shrinking hepatocytes (eosinophilic councilman bodies) were seen. No mononuclear or polymorphonuclear cell infiltrates were observed. Finally, portal terminal venules appeared congested with red blood cells (Fig. 5*C*), a finding that could explain the trabecular fishnet macroscopic appearance of the liver surface (see Fig. 3*C, left*).

Protocol B. Microscopic liver examination, performed in four animals who died spontaneously after the second decom-

tapraid4/zh6-areg/zh6-areg/zh600810/zh67282d10z | xppws | S 1 | 5/26/10 | 2:44 MS: R-00699-2009 Ini: 08/bar/ss

COLOR

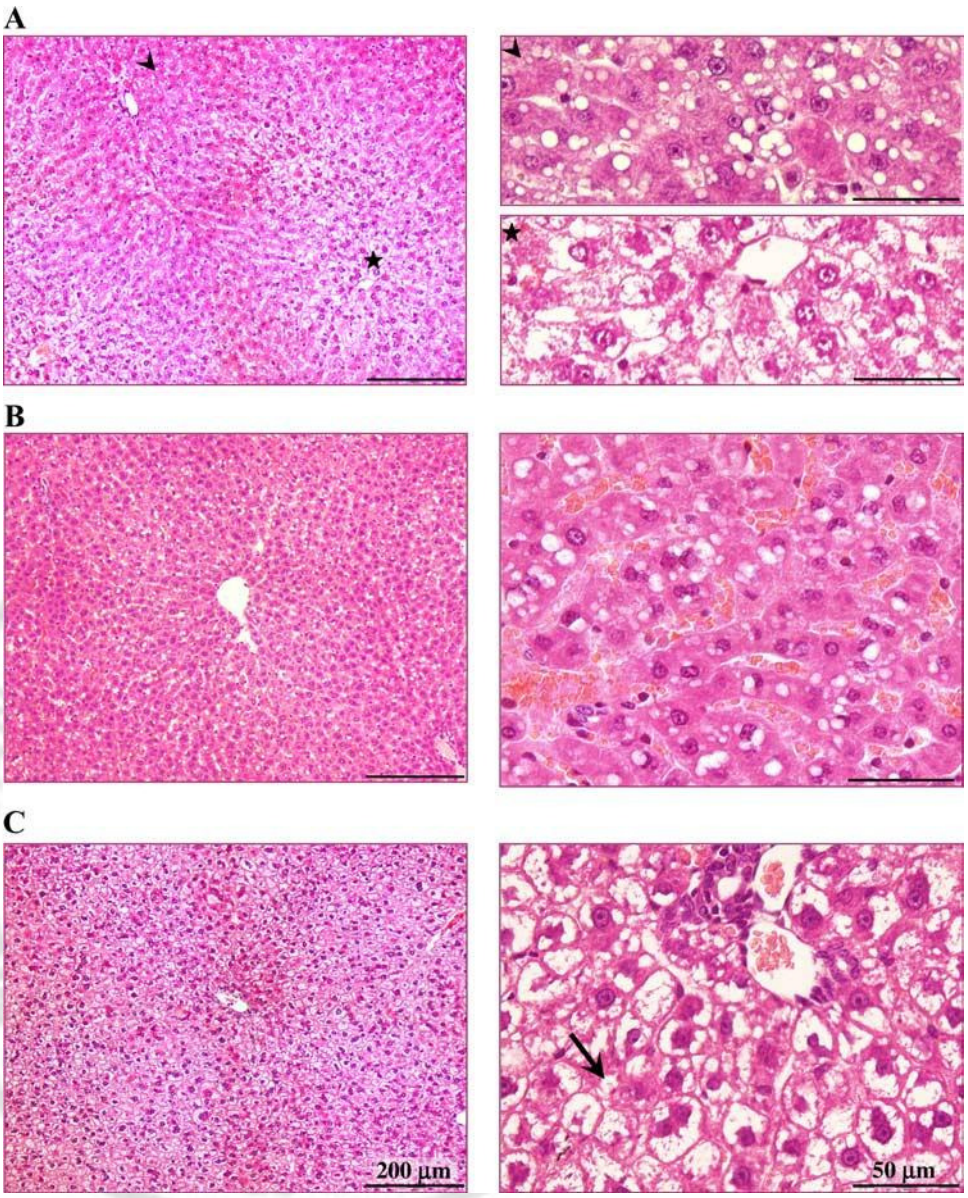

Fig. 5. *Protocol A*: liver histology (hematoxylin and eosin staining). *Left:* low magnification (100) (calibration bar, 200 m). *Right*: high magnification (400) (calibration bar, 50 m). *A*: representative case from *group I* (early spontaneous death following decompression). *Left*: centrilobular hydropic degeneration (arrowhead) associated with severe perilobular vacuolization (star). *Right*: unstained round cavities 2–20 m in diameter in the perilobular zone both within the cells and in the interstitium (*top*), and centrilobular hepatocytes showing hydropic degeneration (*bottom*) are evident at high magnification of the areas marked by the arrowhead and star in the left panel. *B*: representative case from *group II* (killed at 3 h after decompression). *Left*: at low magnification, the perilobular zonation of round, unstained cavities is evident, as well as the intact lobule architecture. *Right*: microcavities 2–20 m in diameter are mostly found within normal-appearing hepatocytes, while sinusoids are congested. *C*: case from *group III* (killed at 24 h). *Left*: severe hydropic degeneration with no zonal distribution, congested portobiliary spaces, collapsed sinusoids, and compressed central veins. *Right*: enlarged view of periportal hepatocytes showing severe hydropic degeneration and scanty hepatocellular lysis (arrow).

pression, showed in all of them moderate-to-diffuse hydropic degeneration either with no zonal distribution or prominently mid- and centrilobular degeneration, associated with mild focal centrilobular necrosis in one animal. Few large cavities (100 to 200 m in diameter) adjacent to perilobular venules and compressing surrounding hepatocytes were also found in one case (Fig. 7*A*). This pattern suggests the persistence of entrapped gas in the liver as encapsulated cavities partially filled with plasma fluid.

In the only surviving rat in this series, focal centrilobular necrosis associated with diffused hydropic degeneration, was present with early remodeling of trabecular structure by initial fibrosis (Fig. 7, *B–D*). No mononuclear or polymorphonuclear cell infiltrates were observed in any animal.

Protocol C. In the eight surviving rats, microscopic examination revealed either no hepatocellular changes (4 cases) or mild (10 vacuoli/100 m^2) intracellular microvacuolization (unstained vacuoli with hematoxylin and eosin, PAS, or red oil) strictly in the perilobular zone (Fig. 7, *E* and *F*).

DISCUSSION

We were able to document the occurrence of gas embolization in the liver following simulated diving and rapid decompression. Only a few older reports have described large bubbles either in the portal vein or in the liver, in animal models of DCS. The apparently low incidence of the phenomenon led to the conclusion that the intestine may serve as a gaseous exchanger for nitrogen elimination rather than as a potential source of gas embolism (1, 23). Actually, this optimistic view is quite widespread among scuba divers, and text books of underwater and hyperbaric medicine do not treat liver gas embolization as a possible complication of scuba diving nor as a component of DCS. We obtained evidence of consistent liver embolization in a rat model of DCS, previously employed by Wisloff and Brubakk (26) to investigate postdecompression gas bubble formation in the systemic circulation by means of ultrasound imaging of the right heart cavities.

tapraid4/zh6-areg/zh6-areg/zh600810/zh67282d10z | xppws | S 1 | 5/26/10 | 2:44 MS: R-00699-2009 Ini: 08/bar/ss

COLOR

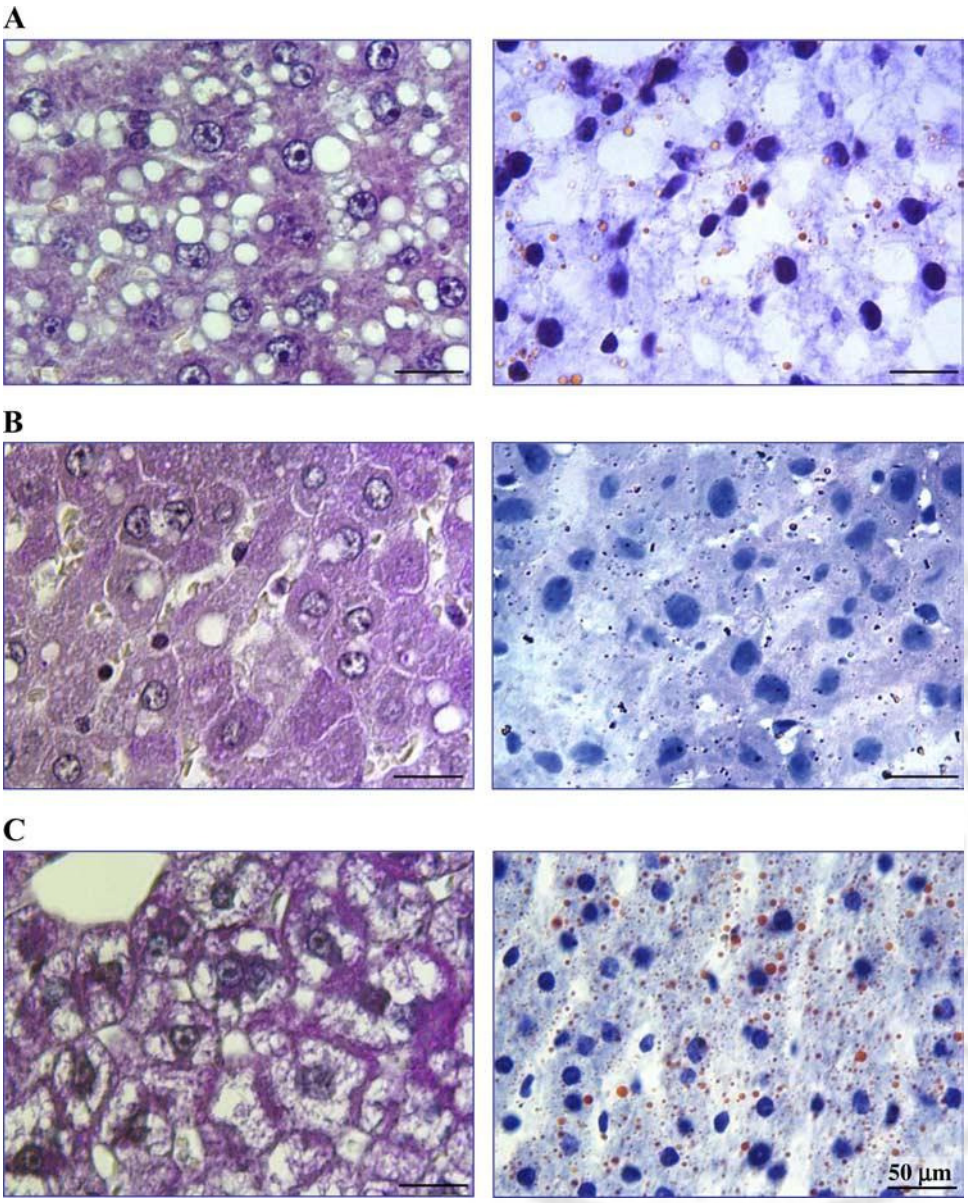

Fig. 6. *Protocol A*: liver histology [periodic acid Shiff staining (PAS) and red oil, magnification, 400; calibration bars, 50 m]. *A*: *group I* PAS (*left*) and red oil (*right*) negative intracellular round microcavities. *B*: *group II* PAS and red oil negative microcavities. *C*: *group III* PAS-positive isolated centrilobular cells and red oil-positive intracellular microvesicles.

In agreement with these authors, the death rate in our study was 50%. In spite of a selected population of animals (all females, small weight range, same diet, same environmental conditions), death was unpredictable and only occurred in the first hour (88% in the first 10 min). Even a pair of animals exposed to the same compression-decompression session underwent different and unpredictable outcomes. The reason(s) for this discrepancy remain unknown and deserve further study. In addition, we exposed 14 animals to the same dive profile twice, 48 h apart. Six out of the seven animals surviving the first decompression died following the second one with an overall mortality rate of 93%. Interestingly enough, this finding rules out the occurrence in the Wistar rat strain of individual animals resistant (or susceptible) to gas embolization.

At gross macroscopy, the spontaneously deceased animals showed a massive presence of gas in the systemic venous circulation as well as in the aorta, possibly due to pulmonary barotrauma (4), a finding that easily explains sudden death. However, this was not the case in surviving animals that showed clear evidence of intrahepatic gas accumulation at 3 h necroscopy.

Gas Bubble Dynamics and Liver Embolism

The presence in early deceased animals of gas bubbles on the intestinal surface and in mesenteric veins, periportal space, and sinusoids, along with their absence in the spleen, strongly indicates that the intestine is the major source of gas for liver embolization. A similar but milder picture was evident in surviving animals killed at 3 h. In conclusion, macro- and micromorphological observations suggest that gas drained from the intestinal wall (where large bubbles were visible even on the surface) into intestinal veins and became visible in the mesenteric veins as long, cylindrical empty spaces interrupting the blood column. Bubbles traveling across the portal terminal veins primarily embolize the periportal zone of hepatic lobules and lodge in the proximal portion of the sinusoids. Trapping of

tapraid4/zh6-areg/zh6-areg/zh600810/zh67282d10z | xppws | S 1 | 5/26/10 | 2:44 MS: R-00699-2009 Ini: 08/bar/ss

COLOR

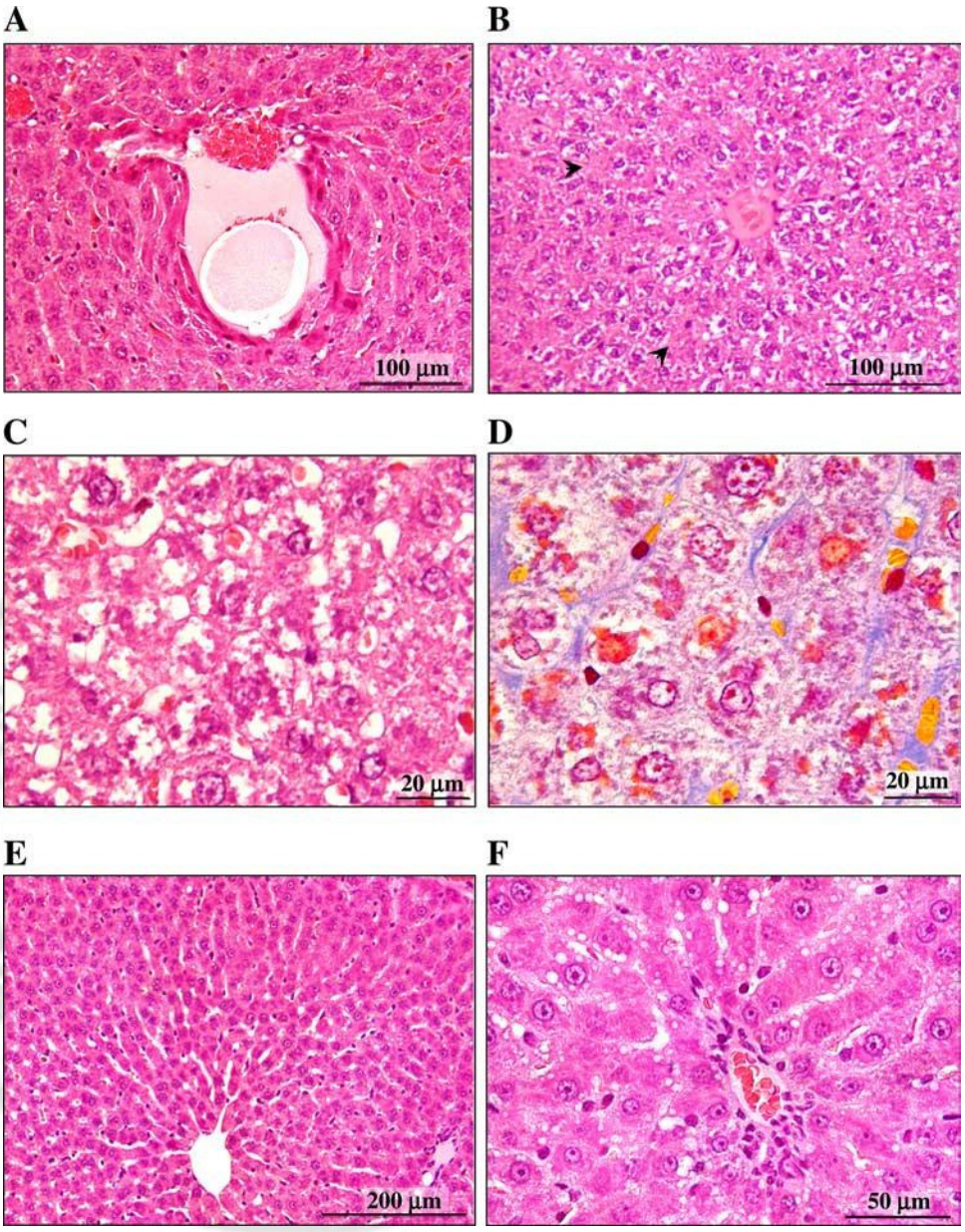

Fig. 7. *A–D*: liver histology from p*rotocol B* (hematoxylin and eosin staining). *A–B:* low magnification, 100; calibration bar, 100 m. *C–D*: high magnification, 400; calibration bar, 20 m. *A*: perilobular large cavity encapsulated by compressed hepatocytes in early spontaneous death following decompression. *B–D*: focal centrilobular necrosis associated with diffused hydropic degeneration (*B* and *C*) and mild fibrosis [stained in blue with Mallory trichromic (*D*)] in the rat that survived in *protocol B*. Arrowheads indicate necrotic zones. *E* and *F*: liver histology from *protocol C* (hematoxylin and eosin staining). *E*: magnification, 100; calibration bar, 200 m. *F*: magnification, 400; calibration bar, 50 m. Intracellular microvacuolization in the strictly perilobular zone is shown in a representative case of surviving animals.

gas bubbles within the liver microcirculation is also evident at 3 h. These findings demonstrate the efficacy of the filtering properties of the hepatic microvasculature for embolizing gas bubbles. Long-lasting mechanical obstruction of sinusoids would cause portal flow impairment and possibly ischemia.

The gaseous nature of interstitial and intracellular cavities observed in the present study cannot be stated with certainty, in spite of the fact that all of our attempts to stain its contents failed, even in cryoslices. Relevant to this matter might be the description of encapsulated, gas-filled cavities in the liver in some stranded cetaceans. The nature of such cavities is still controversial, although some authors consider this peculiar feature the anatomical fingerprint of a particular type of DCS resulting from the animal exposure to midrange sonar and consequent formation of bubbles in the splanchnic district, possibly in response to either rapid decompression or acoustic exposure of nitrogen-supersaturated tissues (8, 16).

Functional and Pathologic Consequences of Liver Embolism

In animals with a single exposition to decompression, histological findings and analysis of marker enzymes of liver damage suggest different time courses of liver gas embolism and hepatocellular injury. Although a massive portal, liver, and systemic venous embolization was present in early-dying animals, microbubbles could be found even 3 h after decompression in surviving rats. Liver cell damage, on the other hand, was minimal at 3 h, while it was present in all cases at 24 h after decompression, although with a wide range of severity (from mild vacuolization to diffuse hydropic degeneration). Only a single case of spontaneous early death showed a pattern of hydropic degeneration with centrilobular zonation, while no lesions were generally associated with the presence of peripportal stainless microcavities. However, when the same decompression protocol was repeated after 48 h (*protocol B*) severe

tapraid4/zh6-areg/zh6-areg/zh600810/zh67282d10z | xppws | S 1 | 5/26/10 | 2:44 MS: R-00699-2009 Ini: 08/bar/ss

hydropic degeneration, both zonal and diffuse, was invariably present as well as focal centrilobular necrosis in two cases and associated with initial fibrosis in the only surviving animal of this series. Thus, repeated exposition enhanced microscopic liver damage.

Among the hematochemical markers analyzed, only the enzymes of liver damage (AST, ALT, and GGT) showed significant changes after decompression. AST and ALT have long been used as sensitive and reliable indicators of liver diseases and are routinely used as clinical endpoints indicative of hepatotoxicity. Of the two, ALT is considered the most liver-specific enzyme in rat injury as it is present mainly in the cytosol of the liver but in low concentrations elsewhere; it is used as marker of hepatocellular necrosis or increased cell membrane permeability (3, 7). AST has cytosolic and mitochondrial forms, and its activity is high in rat liver and also in kidney, pancreas, and erythrocytes (25); thus elevated serum AST is indicative of tissue and cellular damage without specificity for hepatotoxicity.

The findings of the present study are qualitatively in agreement with previous results of experimental studies on liver ischemia of short duration in the rat (22); the lower levels of AST and especially ALT in our study might be the consequence of milder, possibly heterogeneous and discontinuous, ischemic stimulus by microvascular gas embolism, provoking cellular injury but not necrosis. This view seems supported by the presence of vacuolization and cellular hydropic degeneration at histology, which is the result of defects in membrane and/or mitochondrial function, secondary to intracellular ATP depletion. This feature is common to several hepatic injuries including ischemia. It is well known that hepatic cells, especially those of zone 3 (centrilobular), may tolerate relatively long periods of low oxygenation without being irreversibly damaged (17); the usual pathological consequence of a short, reversible ischemic damage is cellular edema and hydropic degeneration (13). Although this type of injury is potentially reversible, it can also lead to hepatocellular lysis, ballooning degeneration, hepatocyte shrinkage (eosinophilic "councilman bodies"), and finally, coagulative necrosis with final replacement by inflammatory cells. Following a single decompression (*protocol A*), we did not observe hepatocellular necrosis even 24 h after gas embolism, in contrast with studies of experimental ischemia induced by clamping of the hepatoduodenal ligament for 30 min or longer, where focal hepatocellular necrosis was detected much earlier than 24 h after reperfusion (11). On the other hand, hepatic glycogen stores were totally depleted in early-dying animals, while they were partially replete at 24 h after decompression, a finding in agreement with other studies of experimental liver ischemia (5).

Histological analysis evidenced minimal-to-mild perilobular cellular swelling and vacuolization at 3 h postdecompression. This picture evolved to perilobular or total lobular hydropic degeneration at 24 h. One can speculate that the consequence of portal venule and sinusoid obstruction, by gas microbubbles formed for a relatively long time after rapid decompression, is a mild, patchy, and discontinuous impairment of blood flow supply to hepatocytes, which would cause potentially reversible hepatocellular damage progressing from perilobular to centrilobular cells. However, the possibility that gas embolism may indirectly induce cellular damage by activating plasma factors of inflammatory response (such as cytokines, TNF- , etc.) (10, 14, 18), as well as a systemic stress response, should also be considered . As a matter of fact, the evidence of centrilobular necrosis at 24 h in two cases of repeated rapid decompression (*protocol B*) strongly suggests that repeated hepatic injury by gas embolism can lead to cellular death and fibrosis. On the other hand, repeated decompressions using a mitigated dive profile (*protocol C*) were unable to elicit significant hepatocellular damage at 24 h after the last procedure and produced, at most, mild cellular microvacuolization similar to that observed at 3 h in *protocol A*. Despite minimal or no cellular changes, however, enzymatic markers of liver injury resulted, elevated also in this group (with an apparent trend toward smaller changes with the number of expositions).

Limits of the Study

According to previous results from other laboratories (26), rat exposure to rapid decompression appears to be characterized by a binary outcome (fulminant DCS or survival without apparent distress, with almost equal chance). This peculiarity may collocate the experimental model far from the human diving condition, due to the unsafe ascent profile. However, the primary aim of our study was to prove that the intestine does not protect the liver from postdiving embolization as generally assumed. To this purpose, we investigated the occurrence of liver embolism in a condition of well-documented systemic gas embolism, as it was the case of the rat model and decompression profile adopted by Wisloff and Brubakk (26). Even considering the surviving animals alone, the conclusion of the study is that the liver is actually a target organ of splanchnic gas embolization following decompression and that the intestine is the primary source of embolizing microbubbles. Actually, even reducing the severity of dive profile, and thus related mortality, from 50% after a single decompression (*protocol A*) to 20% after three decompressions (*protocol C*), liver functional alterations were still evident. Thus, even considering safer decompression profiles, the liver should be considered a potential target of embolism not differently from the lung.

The methodology used in our study prevented us from investigating the dynamics of bubble formation and dissolution as well as the progression of liver damage over time, in single cases. Similarly, we could not correlate the type and extent of liver injury observed at 3 h and 24 h after decompression to the severity and the duration of initial liver embolism. The absence of a longer observation time after single or repeated decompressions limits the conclusions on the long-term outcome of potentially reversible liver damage observed at 24 h.

There is additional uncertainty about the duration of the microbubbles trapped in the liver. The Epstein-Plesset formula on microbubble dissolving time in water and solutions states that 10 m and 100 m bubbles last only 6 s and 600 s, respectively (2, 9). We found bubbles in the sinusoids at 3 h following decompression, and no data are available from the present study regarding the time and dynamics of bubble formation in the intestine during the first few hours after rapid decompression.

Finally, our study does not determine whether intestinal gas has contributed along with respiratory gases, and in what proportion, to the composition of the observed portal microbubbles.

tapraid4/zh6-areg/zh6-areg/zh600810/zh67282d10z | xppws | S 1 | 5/26/10 | 2:44 MS: R-00699-2009 Ini: 08/bar/ss

Clinical Implications

Hepatic portal venous gas is an unusual and unfavorable clinical entity, recognized in recent years as the result of the diagnostic diffusion of ultrasounds and computed tomography, in association with ischemic and nonischemic bowel diseases (19, 21). In contrast, only scanty and contradictory findings on portal, mesenteric, liver, and spleen gas embolism, as well as on abnormal blood markers of liver dysfunction, have been reported in DCS (2, 4, 15, 20), favoring the firm belief that the liver is not a target organ of DCS.

In an experimental model, our study results document the occurrence of liver gas embolisms after rapid decompression, which induce functional and morphological organ alterations. Based on these results, the liver cannot be considered immune from damage related to scuba diving and stressful dive profiles or unsafe decompression. Even if reversible, repeated hepatic injury could lead to liver dysfunction, being this hypothesis is particularly pertinent to professional divers.

A prudent policy for safe diving would require short- and long-term studies on putative liver dysfunction in subjects exposed to decompression.

Perspectives and Significance

This is the first report documenting extensive gas bubble embolism in the liver occurring after rapid decompression not differently from the lung. However, compared with the lung, embolizing bubbles in the liver may persist for a much longer time and produce tissue damage. Although we observed significant cellular necrosis only in few cases of repeated severe decompression and inflammatory response in none, zonal or diffuse hepatocellular damage was clearly evident from 3 h to 24 h after decompression, associated with a significant increase in enzymatic markers of liver damage. Thus, liver cannot be considered, as generally conceived, immune from DCS gas embolism as the result of gas escape into the intestine. Based on these results, the occurrence of liver embolism and its pathological consequences on liver function in human DCS or even outside DCS should be carefully sought and clinically evaluated.

ACKNOWLEDGMENTS

The authors wish to express their gratitude to Drs. A. Piersigilli and A. Pucci for their help in interpreting histological findings.

GRANTS

The work was supported by the CNR Institute of Clinical Physiology, Pisa, the Master in Underwater and Hyperbaric Medicine, and the EXTREME Centre of the Scuola Superiore Sant'Anna, Pisa, Italy.

DISCLOSURES

No conflicts of interest, financial or otherwise, are declared by the author(s).

REFERENCES

1. **Antopol W, Kalberer J, Jr, Kooperstein S, Sugaar S, Chryssanthou C.** Studies on Dysbarism I. Development of decompression syndrome in genetically obese mice. *Am J Pathol* 45: 115–127, 1964.
2. **Barak M, Katz Y.** Microbubbles pathophysiology and clinical implications. *Chest* 128: 2918 –2932, 2005.
3. **Boyd JW.** The mechanisms relating to increases in plasma enzymes and isozymes in diseases of animals. *Vet Clin Pathol* 12: 9 –24, 1983.
4. **Butler BD, Fife C, Sutton T, Pogodsky M, Chen P.** Hepatic portal venous gas with hyperbaric decompression: ultrasonographic identification. *J Ultrasound Med* 14: 967–70, 1995.
5. **Caraceni P, Nardo B, Domenicali M, Turi P, Vici M, Simoncini M, De Maria N, Trevisani F, Van Thiel DH, Derenzini M, Cavallai A, Bernardi MM.** Ischemia-reperfusion injury in rat fatty liver: role of nutritional status. *Hepatology* 29:1139 –1146, 1999.
6. **Carturan D, Boussuges A, Vanuxem P, Bar-Hen A, Burnet H, Gardette B.** Ascent rate, age, maximal oxygen uptake, adiposity, and circulating venous bubbles after diving. *J Appl Physiol* 93: 1349 –1356, 2002.
7. **Clampitt RB, Hart RJ.** The tissue activities of some diagnostic enzymes in ten mammalian species. *J Comp Pathol* 88: 607–621, 1978.
8. **Cox TM, Ragen TJ, Read AJ, Vos E, Baird RW, Balcomb K, Barlow J, Caldwell J, Cranford T, Crum L, D'Amico A, D'Spain G, Fernández A, Finneran J, Gentry R, Gerth W, Gulland F, Hildebrand J, Houserp D, Hullar T, Jepson PD, Ketten D, Macleod CD, Miller P, Moore S, Mountain DC, Palka D, Ponganis P, Rommel S, Rowles T, Taylor B, Tyack P, Wartzok D, Gisiner R, Meads J, Benner L.** Understanding the impacts of anthropogenic sound on beaked whales. *J Cetacean Res Manage* 7: 177–187, 2006.
9. **Epstein PS, Plesset MS.** On the stability of gas bubbles in liquid-gas solutions. *J Chem Phys* 18: 1505–1509, 1950.
10. **Ersson A, Walles M, Ohlsson K, Ekholm A.** Chronic hyperbaric exposure activates proinflammatory mediators in humans. *J Appl Physiol* 92: 2375–2380, 2002.
11. **Gujral JS, Bucci TJ, Farhood A, Jaeschke H.** Mechanism of cell death during warm hepatic ischemia reperfusion in rats: apoptosis or necrosis? *Hepatology* 33: 397–405, 2001.
12. **Hedin PA.** Gastrointestinal gas production in rats as influenced by some animal and vegetable diets, sulfiting and antibiotic supplementation. *J Nutr* 77: 171–176, 1962.
13. **Hu GH, Lü XS.** Effect of normothermic liver ischemic preconditioning on the expression of apoptosis-regulating genes C-jun and Bcl-XL in rats. *World J Gastroenterol* 11: 2579 –2582, 2005.
14. **Huang KL, Wu CP, Chen YL, Kang BH, Lin YC.** Heat stress attenuates air bubble-induced acute lung injury: a novel mechanism of diving acclimatization. *J Appl Physiol* 94: 1485–1490, 2003.
15. **Jauchem JR, Waligora JM, Conkin J, Horrigan DJ Jr, Johnson PC Jr.** Blood biochemical factors in humans resistant and susceptible to formation of venous gas emboli during decompression. *Eur J Appl Physiol* 55: 68 –73, 1986.
16. **Jepson PD, Arbelo M, Deaville R, Patterson IAP, Castro P, Baker JR, Degollada E, Ross HM, Herráez P, Pocknell AM, Rodríguez F, Howie FE, Espinosa A, Reid RJ, Jaber JR, Martin V, Cunningham AA, Fernández A.** Gas-bubble lesions in stranded cetaceans. *Nature* 425: 575–576, 2003.
17. **Malarkey DE, Johnson K, Ryan L, Boorman G, Maronpot RR.** New insights into functional aspects of liver morphology. *Toxicol Pathol* 33: 27–34, 2005.
18. **Nyquist PA, Dick EJ Jr, Buttolph TB.** Detection of leukocyte activation in pigs with neurologic decompression sickness. *Aviat Space Environ Med* 75: 211–214, 2004.
19. **Peloponissios N, Halkic N, Pugnale M, Jornod P, Nordback P, Meyer A, Gillet M.** Hepatic portal gas in adults: review of the literature and presentation of a consecutive series of 11 cases. *Arch Surg* 138:1367–70, 2003.
20. **Philp RB, Freeman DJ, Francey I.** Hematology and blood chemistry in saturation diving: II. Open sea versus hyperbaric chamber. *Undersea Biomed Res* 2: 251–265, 1975.
21. **Schindera ST, Triller J, Vock P, Hoppe H.** Detection of hepatic portal venous gas: its clinical impact and outcome. *Emerg Radiol* 12: 164 –70, 2006.
22. **Serafin A, Rosello-Catafau J, Prats N, Xaus C, Gelpi E, Peralta C.** Ischemic preconditioning increases the tolerance of fatty liver to hepatic ischemia-reperfusion injury in the rat. *Am J Pathol* 161: 587–601, 2002.
23. **Shim SS, Patterson FP, Kendall MJ.** Hyperbaric chamber and decompression sickness: an experimental study. *Canad Med Ass J* 97: 1263–1272, 1967.
24. **Su CL, Wu CP, Chen SY, Kang BH, Huang KL, Lin YC.** Acclimatization to neurological decompression sickness in rabbits. *Am J Physiol Regul Integr Comp Physiol* 287: R1214 –R1218, 2004.
25. **Tennant B.** Hepatic function. In: *Clinical Biochemistry of Domestic Animals* (5th ed.), edited by Kaneko JJ, Harvey JW, Bruss ML. Toronto: Academic, 1997, p. 327–352.
26. **Wisloff U, Brubakk AO.** Aerobic endurance training reduces bubble formation and increases survival in rats exposed to hyperbaric pressure. *J Physiol* 537: 607–611, 2001.